Chinese Journal of Polymer Science Vol. 31, No. 5, (2013), 798–808

Chinese Journal of Polymer Science

MOLECULAR WEIGHT DEPENDENCE OF CRYSTAL PATTERN TRANSITIONS OF POLY(ETHYLENE OXIDE)*

Guo-liang Zhang, Liu-xin Jin, Ping Zheng and Wei Wang**
Center for Synthetic Soft Materials, The Key Laboratory of Functional Polymer Materials of Ministry of Education and Institute of Polymer Chemistry, College of Chemistry, Nankai University, Tianjin 300071, China
Xiao-jing Wen
School of Resources and Materials, Northeastern University at Qinhuangdao, Qinhuangdao 066004, China

Abstract Crystal patterns in ultrathin films of six poly(ethylene oxide) fractions with molecular weights from 25000 to 932000 g/mol were characterized within crystallization temperature range from 20 °C to 60 °C. Labyrinthine, dendritic and faceted crystal patterns were observed in different temperature ranges, and then labyrinthine-to-dendritic and dendritic-to-faceted transition temperatures $T_{L\text{-}D}$ and $T_{D\text{-}F}$ were quantitatively identified. Their molecular weight dependences are $T_{L\text{-}D}(M_w) = T_{L\text{-}D}(\infty) - K_{L\text{-}D}/M_w$, where $T_{L\text{-}D}(\infty)$ = 38.2 °C and $K_{L\text{-}D}$ = 253000 °C·g/mol and $T_{D\text{-}F}(M_w) = T_{D\text{-}F}(\infty) - K_{D\text{-}F}/M_w$, where $T_{D\text{-}F}(\infty)$ = 54.7 °C and $K_{D\text{-}F}$ = 27000 °C·g/mol. Quasi two-dimensional blob models were proposed to provide empirical explanations of the molecular weight dependences. The labyrinthine-to-dendritic transition is attributed to a molecular diffusion process change from a local-diffusion to diffusion-limited-aggregation (DLA) and a polymer chain with $M_w \approx 253000$ g/mol within a blob can join crystals independently. The dendritic-to-faceted transition is attributed to a turnover of the pattern formation mechanism from DLA to crystallization control, and a polymer chain with a $M_w \approx 27000$ g/mol as an independent blob crosses to a depletion zone to join crystals. These molecular weight dependences reveal a macromolecular effect on the crystal pattern formation and selection of crystalline polymers.

Keywords: Poly(ethylene oxide); Crystallization; Pattern formation; Transition; Molecular weight dependence.

INTRODUCTION

Two major tasks of polymer science focus on creating macromolecules with large enough molecular weights by polymerization and on understanding the molecular weight dependence of polymer properties. It is well-known that most properties of polymers are molecular-weight-dependent, which is a unique feature completely different from other materials. Typical examples are the scaling relation between melt viscosity and weight-average molecular weight $\eta_0 \propto M_w^{\alpha}$, in which $\alpha = 3.4$, stemming from the entanglement of long polymer chains[1], and the Flory-Fox equation $T_g = T_g(\infty) - K/M_n$, a simple empirical formula that relates molecular weight to the glass transition temperature, T_g, of a polymer system due to the chain end effect[2].

Polymer crystallization is one of the most intriguing topics in macromolecule science and even condensed matter physics[3–5]. Nowadays, we know well that crystalline polymer chains kinetically prefer to fold several times to form metastable folded-chain lamellar crystals under supercooled conditions. Molecular diffusion rate, R_d, and crystal growth rates, R_c, cooperatively influence polymer crystallization behaviors[6–14]. When

* This work was financially supported by the National Science Foundation of China (No. 20874053).
** Corresponding author: Wei Wang (王维), E-mail: weiwang@nankai.edu.cn
Invited paper dedicated to Professor Fosong Wang on the occasion of his 80th birthday
Received December 20, 2012; Revised January 28, 2013; Accepted February 1, 2013
doi: 10.1007/s10118-013-1273-0

crystallization temperatures (T_cs) close to T_g, $R_c >> R_d$ [6, 10, 12]. Actually, crystallization occurring under such conditions is governed by a limited diffusion of molecules[14−17]. At the opposite extreme, at high crystallization temperature (T_c), $R_c << R_d$ which means sufficient chain conformational adjustment to form well-defined crystals. In intermediate temperature range, coupling and competition of R_d and R_c have a further effect on crystal textures and morphologies. As a basic way to understand polymer crystallization, studies on crystal morphology have attracted many attentions of polymer physicists. The resultant crystal morphology may encompass information in molecular level and provide insight into the crystal growth process[3].

Polymer crystallization in thin or ultrathin films has been increasingly studied because ultrathin films offer us a quasi-two-dimensional (2D) condition to study the crystallization behaviors of mono-lamella crystals[14, 18−40]. Mono-lamella crystals may provide us more information to understand polymer crystallization that we cannot obtain from the studies on spherulites in bulk samples. Since R_d and R_c are highly dependent on T_c, the crystal patterns can be manipulated easily by tuning T_c. Labyrinthine, dendritic, seaweed, compact and faceted crystal patterns have been found in crystalline polymer ultrathin films[14, 19, 20, 27, 29−34, 36, 39]. In a low T_c range, dendritic and seaweed crystals have been commonly observed[19, 20, 27, 29−31, 36], reflecting a governing mechanism of diffusion-limited-aggregation (DLA) with and without anisotropic growth[41]. Within a high T_c range, faceted crystals have been usually observed[20, 27, 30, 31, 36], meaning that nucleation-limited-growth (NLG) mechanism is dominant. When DLA and NLG mechanisms couple together, a compact structure would form[27, 30−32]. More importantly, many efforts have been devoted to study the transitions among different crystal patterns to get a complete morphology diagram[27, 30, 32, 42], which help us deeply understand the essential relationship between crystallization and pattern formation mechanisms.

Considering the macromolecular effect on polymer crystallization and diffusion, it is well known that R_d and R_c are also highly dependent on molecular weight, thus the crystal patterns of crystalline polymers can be manipulated by tuning molecular weight as well. In previous work, we have done systematical studies on the pattern formation and selection of ten poly(ethylene oxide) (PEO) fractions with molecular weights ranged from 2000 g/mol to 932000 g/mol[14, 26, 27, 29−33, 37]. Several crystal pattern transitions for each PEO fraction have been quantitatively described as a function of T_c[14]. Then, a morphology diagram for the pattern formation and selection of PEO fractions has been constructed by plotting transition temperatures versus molecular weight[32]. Herein, we would like to introduce our study on the molecular weight dependence of the labyrinthine-to-dendritic and dendritic-to-faceted pattern transitions. We will first characterize the diverse crystal patterns of the six PEO fractions ranged from 25000 g/mol to 932000 g/mol in different T_cs, and then quantitatively analyze the labyrinthine-to-dendritic and dentritic-to-faceted crystal pattern transitions and, finally determine the transition temperatures. Interestingly, their molecular weight dependences can be well described using the Flory-Fox-type formula $T = T(\infty) - K/M$ and the values of K parameters suggest that a polymer chain with a critical molecular weight can independently join crystals. Two blob models will be proposed to explain the macromolecular effect of the pattern formation and selection of crystalline polymers.

EXPERIMENTAL

Materials

Six linear PEO fractions were purchased from Polymer Source Inc and Polymer Standards Service GmbH. They are hydroxyl-terminated at one end and methyl-terminated at other end. Their weight-average molecular weight, M_w, the polydispersity index, M_w/M_n and the equilibrium melting temperature, T_m^0, are listed in Table 1. The relatively narrow molecular weight distributions will minimize the effect of polydispersity on the crystal pattern features.

Sample Preparation

Toluene solutions of these PEO fractions with a concentration of *ca*. 0.15 wt% were prepared in glassware respectively. Silicon wafers with a size of about 0.8 cm × 0.8 cm were treated in the Piranha solution of H_2SO_4 (98%):H_2O_2 (30%) = 3:1 at *ca*. 120 °C for 30 min to add a layer of −OH groups at the silicon surfaces and then

cleaned in an ultrasonic water bath. The measured contact angle, θ, of water is θ = 8° for the treated silicon wafers and θ = 55° for the un-treated silicon wafers. Thus the treated surface was hydrophilic, and the interaction between hydrophilic PEO and the treated silicon surface would be very strong. Ultrathin PEO films were prepared by drop-casting the solution (3–4 μL) onto silicon surfaces at room temperature. The samples were dried at ambient condition overnight and then treated in vacuum at room temperature for 12 h. The as-prepared samples were first heated to 80.0 °C for 5 min to form a uniform molten layer with a thickness of 3–4 nm and then were cooled to the specific T_cs to let the supercooled melt recrystallize for 5–12 h.

Table 1. Molecular parameters of the PEO fractions

Samples	M_w (g/mol)	M_w/M_n	T_m^0 (°C)
25k-PEO	25000	1.17	67.4
35k-PEO	35000	1.23	67.8
116k-PEO	116000	1.18	68.6
205k-PEO	205000	1.18	68.8
610k-PEO	610000	1.10	69.0
932k-PEO	932000	1.11	69.0

Instrument

A hot-stage multimode atomic force microscope (AFM, Digital Instrumental Nanoscope IV) was used to visualize crystal patterns in tapping mode.

Image Analysis

The digital AFM images were used to determine the fractal dimension, D_f, of the crystal patterns according to the dilation method. The D_f definition is $N(r) \propto r^{-D_f}$, where N stands for the number of segments and r for the length of segments. With increasing N we can approximate the rough curve length.

RESULTS AND DISCUSSION

Labyrinthine-to-Dendritic Transition

In a recent publication, we have demonstrated that the labyrinthine crystal pattern can appear in thin film samples when M_w is above 25000 g/mol[32]. The AFM images in Fig. 1 display the labyrinthine and dendritic patterns observed in the six PEO fractions within a temperature range from 20 °C to 44 °C. In the low T_c range, the crystal patterns are labyrinthine, as shown in images (a_1)–(a_6) and (b_1)–(b_6). In the relatively high T_c range, the crystal patterns are dendritic, as shown in images (d_1)–(d_6). In the intermediate T_c range, the crystal patterns have mixed features of both the labyrinthine and dendritic patterns, as shown in images (c_1)–(c_6). Clearly, these AFM images show a gradual pattern transition from labyrinthine to dendritic patterns with increasing T_c for these PEO fractions.

Morphological difference between the labyrinthine and dendritic crystal patterns can be quantitatively identified. The labyrinthine pattern has a periodicity in width directions: the identical width of branches and identical distance between parallel neighbors, but, the dendritic crystal has the feature of hierarchical branches. Consequently, these two kinds of crystal patterns can be clearly distinguished using fast Fourier transform (FFT) as shown in Fig. 2. Figure 2(a_1) depicts a typical labyrinthine crystal. Figure 2(a_2) is the 2D intensity pattern (512 × 512 pixels) of Fig. 2(a_1) obtained using FFT. Four strong scattering spots indicate the long period of stripe-like branches in width directions. After azimuthally integrating the intensity, a circularly averaged integral curve can be obtained as shown in Fig. 2(a_3). After subtracting an exponential decay fitting curve in Fig. 2(a_3), the peak area, A, may be obtained in Fig. 2(a_4). As to the dendritic crystal, similar analyses were done as shown in Figs. 2(b_1)–2(b_4). Because of a lacking periodic feature, there are no scattering peaks.

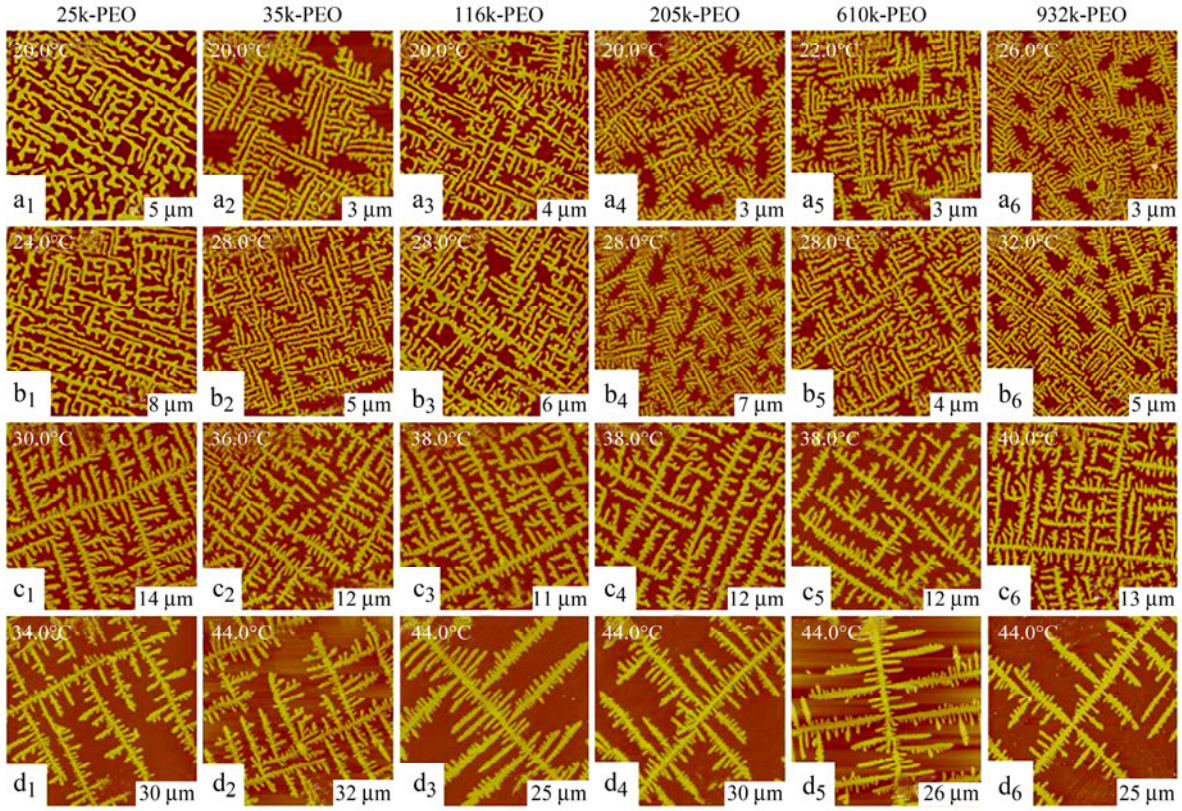

Fig. 1 AFM height images showing the evolution from the labyrinthine crystal pattern to the dendritic crystal pattern as a function of T_c for the six PEO fractions (The length values denoted in the AFM images correspond to the side lengths of the square images.)

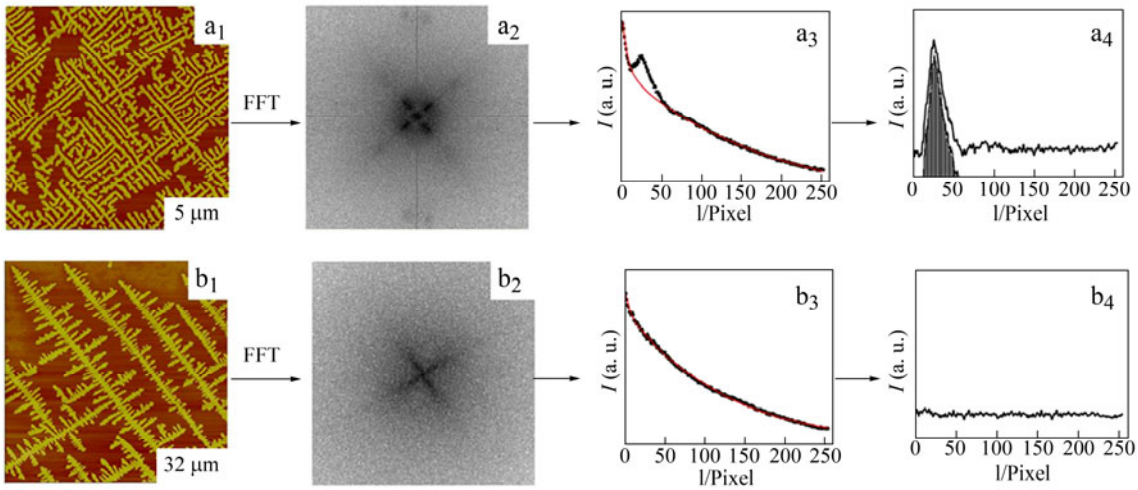

Fig. 2 (a_1 and b_1) Typical labyrinthine and dendritic crystal patterns; (a_2 and b_2) Corresponding 2D FFT patterns; (a_3 and b_3) Circular average integral curves of the 2D FFT patterns, and the red curves are exponential decay fitting results; (a_4 and b_4) Intensity curves after subtracting the exponential decay fitting curves

We note that the peak area, A, for the labyrinthine patterns is almost a constant, and its value gradually decreases to zero with the labyrinthine-to-dendritic pattern transition. The continuous decrease of A indicates a gradual loss of the periodicity. Plotting normalized A value against T_c can quantitatively describe the labyrinthine-to-dendritic transition as shown in Fig. 3. The solid curves in the figure are the fitting results using the Sigmoid function of $A = A_{min} + (A_{max}-A_{min})/(1 + \exp((T_x-T_0)/w))$, where A_{max} means the normalized value for the labyrinthine pattern, $A_{min} \approx 0$ means the value for the dendritic pattern, T_0 means the inflexion temperature and w is the half-width of transition that varies from 0.8 °C to 1.4 °C for the PEO samples. The six curves in Fig. 3 show a similar shape, that is, a similar T_c dependence, indicating an identical mechanism controlling the labyrinthine-to-dendrite transition for the six PEO samples.

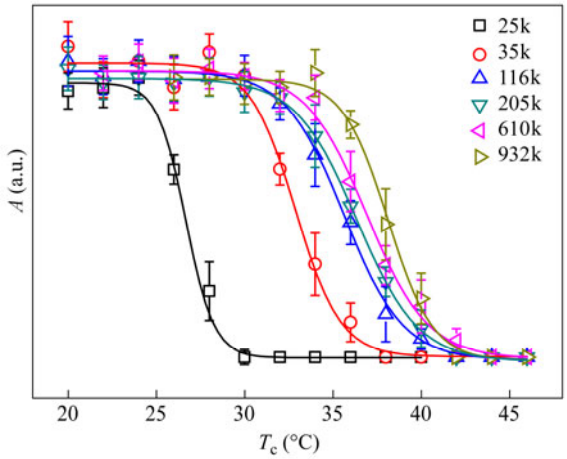

Fig. 3 Plots of A versus T_c for the six PEO fractions

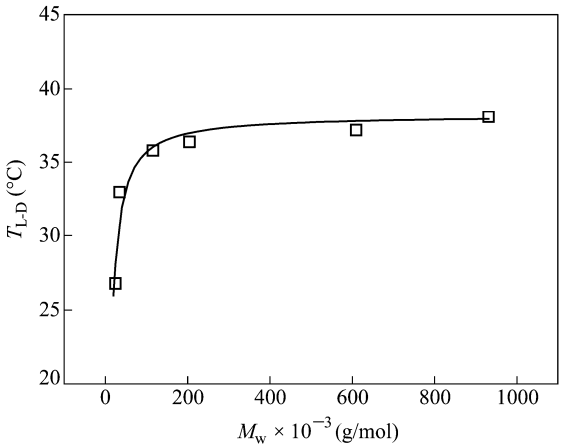

Fig. 4 Plot of $T_{L\text{-}D}$ versus M_w

The inflexion temperature T_0 is selected as the labyrinthine-to-dendritic transition temperature, $T_{L\text{-}D}$. Figure 4 presents the molecular weight dependence of $T_{L\text{-}D}$. At first glance, the relationship between $T_{L\text{-}D}$ and M_w is similar to the Flory-Fox-type equation used to describe the molecular weight dependence of T_g in a polymer system.

$$T_{L\text{-}D}(M_w) = T_{L\text{-}D}(\infty) - K_{L\text{-}D}/M_w \quad (1)$$

where $T_{L\text{-}D}(\infty)$ is the maximum transition temperature at infinite molecular weight and $K_{L\text{-}D}$ is a constant. The solid curve in Fig. 4 is the fitting results using Eq. (1), where $T_{L\text{-}D}(\infty)$ = 38.2 °C and $K_{L\text{-}D}$ = 253000 °C·g/mol. This molecular dependence means that $T_{L\text{-}D}$ increases rapidly with increasing M_w when M_w < 253000 g/mol; whereas it asymptotically approaches to $T_{L\text{-}D}(\infty)$ when M_w > 253000 g/mol. This means that 253000 g/mol is a critical value for the molecular weight dependence of the labyrinthine-to-dendritic transition.

Dendritic-to-Faceted Transition

The AFM images in Fig. 5 show a morphological transition of the PEO crystals from dendritic to faceted patterns for the six PEO fractions. It is worth noting that this dendritic-to-faceted transition appears in the temperature range from 50 °C to 60 °C, higher than that of the labyrinthine-to-dendritic transition. In the images Figs. 5(a_1)–5(a_6) the crystal patterns obtained at T_c = 50 °C are dendritic. The images Figs. 5(b_1)–5(b_6) and 5(c_1)–5(c_6) show the four-fold-symmetric patterns (FFS) obtained in the range of 50 °C ≤ T_c ≤ 57 °C. In the T_c ≥ 57 °C range, the typical faceted crystal patterns are found, as shown in the images Figs. 5(d_1)–5(d_6). Clearly, these AFM images show a gradual pattern transition from the dendritic pattern to the faceted pattern through the FFS pattern with increasing T_c.

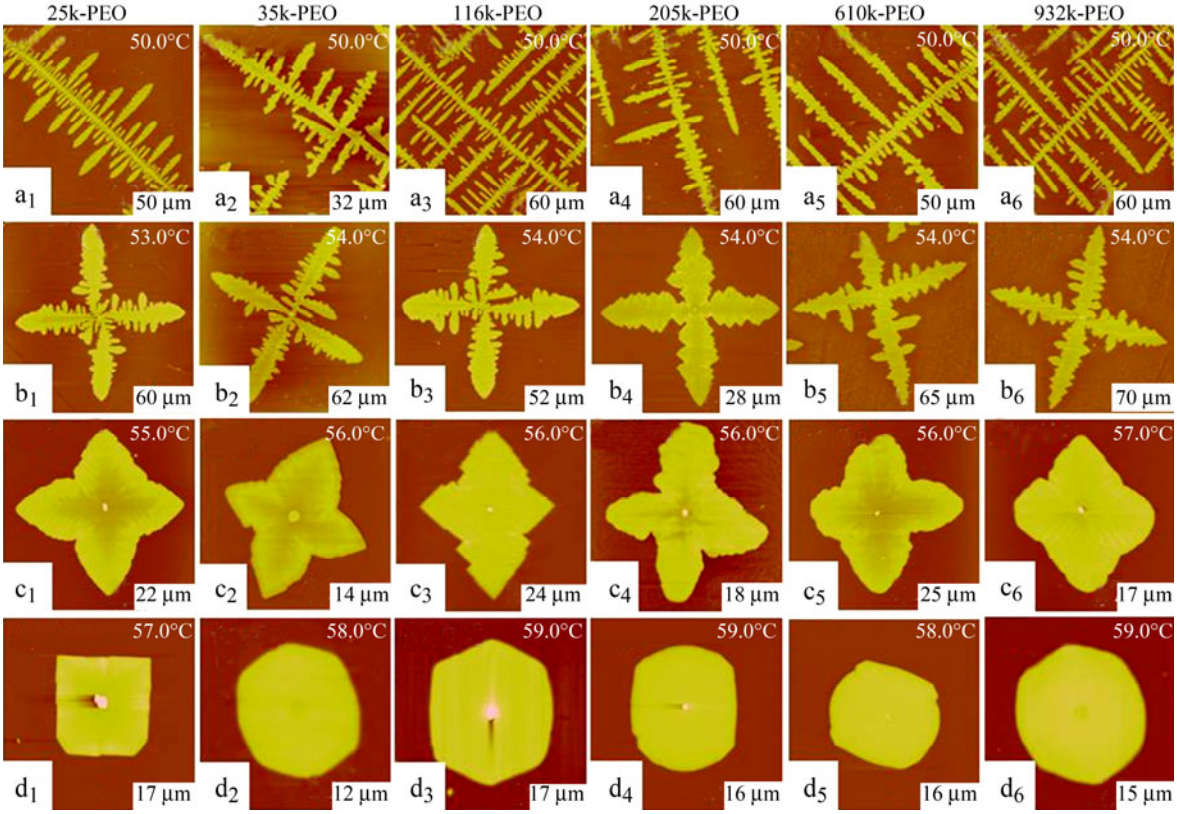

Fig. 5 AFM height images showing the evolution from the dendritic crystal pattern to the faceted crystal pattern through the four-fold-symmetric pattern as a function of T_c for the six PEO fractions (The length values denoted in the AFM images correspond to the side lengths of the square images.)

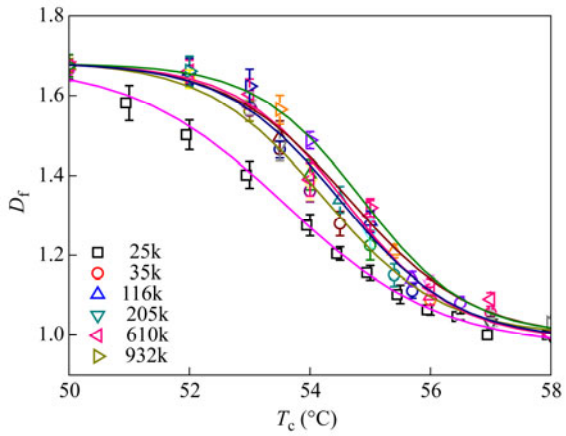

Fig. 6 Plots of D_f versus T_c for the six PEO fractions

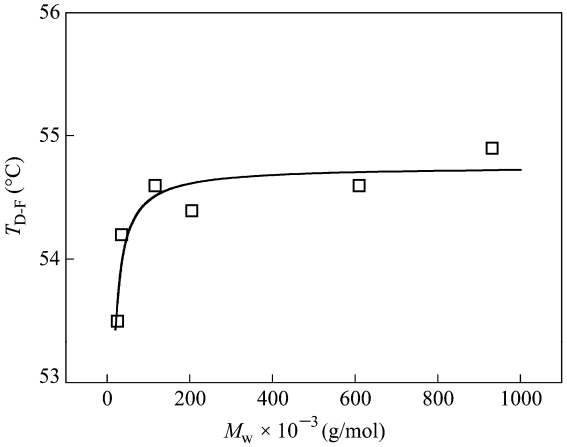

Fig. 7 Plot of T_{D-F} versus M_w

Dendritic crystal patterns can be described by fractal geometry, while faceted crystals may be described by Euclidean geometry. Thus, the dendritic-to-faceted transition can be quantitatively identified by the change of the fractal dimension, D_f, as a function of T_c[30]. Figure 6 displays the plot of D_f versus T_c for the six PEO fractions. The solid curves are the Sigmoidal fitting results and the inflexion temperature T_0 is selected as the dendritic-to-faceted transition temperature, T_{D-F} for each PEO fraction. Figure 7 presents the molecular weight dependence of T_{D-F}. The relationship between T_{D-F} and M_w is also described using the Flory-Fox-type formula.

$$T_{D\text{-}F}(M_w) = T_{D\text{-}F}(\infty) - K_{D\text{-}F}/M_w \quad (2)$$

where $T_{D\text{-}F}(\infty)$ is the maximum transition temperature at infinite molecular weight and $K_{D\text{-}F}$ is a constant. The solid curve in Fig. 7 is the fitting results using Eq. (2), where $T_{D\text{-}F}(\infty)$ = 54.7 °C and $K_{D\text{-}F}$ = 27000 °C·g/mol. This molecular dependence also means that $T_{D\text{-}F}$ increases rapidly with increasing M_w when M_w < 27000 g/mol; whereas it asymptotically approaches to $T_{D\text{-}F}(\infty)$ when M_w > 27000 g/mol. This means that 27000 g/mol is also a critical value for the molecular weight dependence of the dendrite-to-faceted crystal transition.

Molecular Weight Dependence

Most physical properties of polymers, such as radius of gyration of polymer chain, molecular diffusion coefficient, vescoelasticity, crystal growth rate, glass transition temperature, equilibrium melting temperature and mechanical properties are molecular-weight-dependent, the most unique feature of polymeric materials[1]. Interestingly, the molecular weight dependences of the two crystal pattern transition temperaures in this study are the same as the molecular weight dependence of glass transition temperature, described by the Flory-Fox equation $T_g = T_g(\infty) - K_g/M_n$. This simple empirical formula relates molecular weight to T_g of a polymer system due to the chain end effect[2]. $T_g(\infty)$ is an asymptotically limiting glass transition temperature at infinite molecular weight and K_g is a positive constant depending on polymer and means that T_g approaches to the asymptotic limit of $T_g(\infty)$ when M_n of a polymer is larger than the value of K_g. K_g value of PEO is in order of 10^5 [2, 43].

In the Fox-Flory-type Eqs. (1) and (2) we obtained $K_{L\text{-}D}$ = 253000 °C·g/mol and $K_{D\text{-}F}$ = 27000 °C·g/mol for the two pattern transitions. It means that there are two critical molecular weights $M_w \approx$ 253000 g/mol and $M_w \approx$ 27000 g/mol controlling the two transition processes. Below the critical molecular weights, the transition temperatures highly depend on the molecular weight, thus $T_{L\text{-}D}$ and $T_{D\text{-}F}$ increase rapidly with increasing molecular weight. Above the critical molecular weights, the transition temperatures asymptotically approach to the maximum transition temperatures, $T_{L\text{-}D}(\infty)$ or $T_{D\text{-}F}(\infty)$. Therefore, we think that there are two specific structural units with $M_w \approx$ 253000 g/mol and $M_w \approx$ 27000 g/mol. We also notice that the two critical values are much higher than the critical entanglement M_n of 6800 g/mol of PEO in bulk[43]. Certainly, the entanglements between polymer chains will highly affect the diffusion and subsequently influence the crystallization behaviors. It is worth pointing out that in the ultrathin film polymer chains present a "pancake" conformation[44] and entanglement density is reduced.

Mechanisms of the Pattern Transitions

It is well known that molecular diffusion represented by diffusion coefficient, D, and crystal growth rate, R_c, have opposite temperature dependences: D will increase, whereas R_c will decrease with increasing temperature. A characteristic diffusion length, λ, of supercooled material in diffusion field, which is expressed as $\lambda \propto D/R_c$, can provide a semi-quantitative determination of coupling and competition of D and R_c on the pattern formation and selection[7, 45–47]. In this way its value can reason the entire crystallization process as well as the resultant crystal morphology. Its significance can be enlarged in the mono-lamella crystal pattern formation because a depletion zone existing in-between the crystal fronts and amorphous layers will make the diffusion more difficult.

Three drawings in Figs. 8(a_1–c_1) schematically depict a depletion zone existing in-between crystals and amorphous layers. Note that the distance between the tip and the amorphous layer of facing the tip is the shortest. Three AFM images in Figs. 8(a_2–c_2) show the labyrinthine, dendritic and faceted patterns, respectively. Individual chains have to cross the depletion zone to mainly join the crystal tip owing to the shortest distance, thus their diffusion process is one of the key factors controlling the pattern formation and selection. In a low T_c range, diffusion coefficient of supercooled polymer chains is extremely low and crystal growth is very fast, thus, λ is very small. In this case, polymer chains have no ability to diffuse "proactively" across the depletion zone to join the crystal tip. Yet, the rapidly growing crystal tips can attract them passing through the depletion zone and then draw them into the crystals. In other words, polymer chains need only a local-diffusion in the area just

limited in front of individual crystal tips, as indicated in Fig. 8(a_1). Therefore, the labyrinthine crystals with a periodic structure are created, as shown in Fig. 8(a_2)[14].

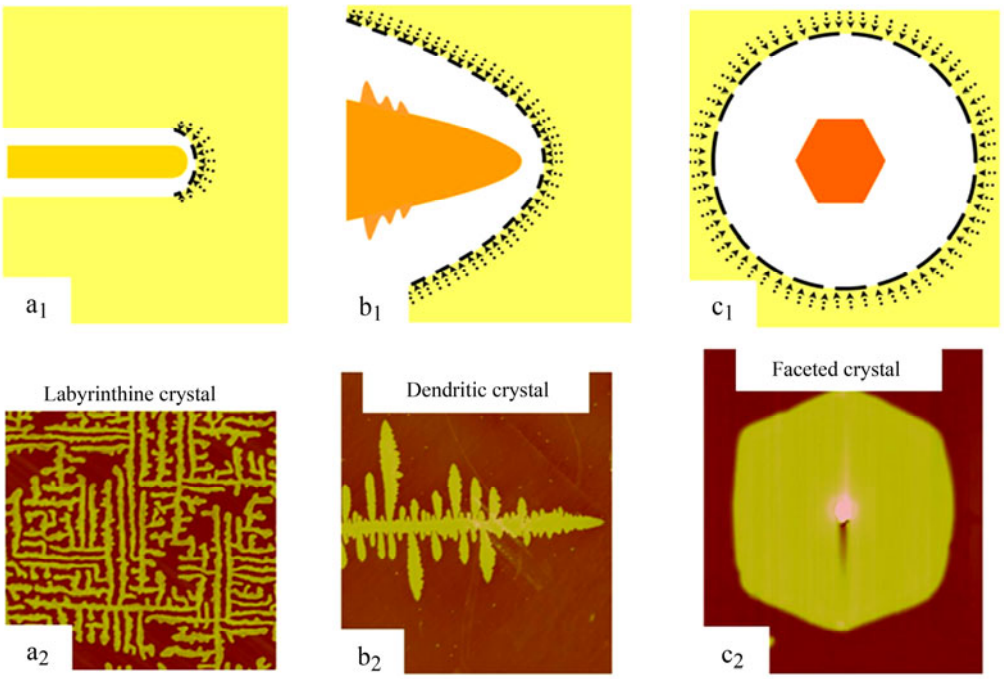

Fig. 8 (a_1) Schematics of molecular local-diffusion ahead of an individual labyrinthine crystal tip; (a_2) Typical labyrinthine crystal pattern; (b_1) Schematics of a diffusion filed ahead of a dendritic crystal tip; (b_2) Typical dendritic crystal pattern; (c_1) Schematics of molecular diffusion around a faceted crystal; (c_2) Typical faceted crystal pattern
Note that a depletion zone, the white area in (a_1–c_1), exists in-between a dark yellow crystal and a light yellow amorphous layer. The distance between the tip and the amorphous layer of facing the tip is shortest.

In a high T_c range, diffusion coefficient of polymer chains is high and crystal growth rate slows down, thus λ increases. It means that polymer chains can take a long range diffusion to enter crystal tips as well as the surrounding area of the crystals, thus the crystals become wider and side-branches can form behind the main growing tip, as indicated in Fig. 8(b_1). This is the DLA mechanism that creates dendritic crystals with hierarchical structures, as shown in Fig. 8(b_2). In an intermediate T_c range, crystal patterns have the mixed feature of both labyrinthine and dendritic crystal patterns. Therefore, the labyrinthine-to-dendritic transition is related to the change of λ with increasing T_c.

With further increasing T_c, diffusion coefficient of polymer chains increases further and crystal growth rate slows down, thus λ becomes very large. It means that polymer chains easily cross the wider depletion zone to come to the perimeter of crystals and then wait for being admitted by the crystals because the sticking probability becomes very low (see Fig. 8c_1). In other words, crystals will highly select polymer chains or a part of them and then let them join in the suitable position with the lowest potential energy. This also means that the nucleation and crystallization on the growth surface of crystals become the dominant step in determination of the crystal pattern formation. Therefore, the formed crystals have the faceted pattern, as shown in Fig. 8(c_2).

Origin of Molecular Weight Dependence of the Pattern Transitions

It is worth mentioning that the T_cs used are higher than T_g (T_g is around −20 °C for PEO thin films on attractive substrate[48]). The molecular weight dependence of $T_{L\text{-}D}$ is partially attributed to the molecular weight dependence of λ. For the labyrinthine crystals the theoretical molecular weight dependences in ultrathin films are

$D \propto M_w^{-1.5}$ and $R_c \propto M_w^{-1.25}$, so $\lambda \propto M_w^{-0.24\pm0.03}$, that is, λ decreases with M_w [14]. Two main reasons that cause the decrease of polymer chain diffusion are: the rapid increases in entanglement density of polymer chains and in the interaction between a single chain and the treated surface of silicon wafer with increasing M_w. To accomplish the labyrinthine-to-dendritic transition, the PEO chains with high M_w will need a high thermal energy, k_BT (where k_B is Boltzmann constant and T is absolute temperature) to drive them to diffuse towards the crystals. Therefore, higher the molecular weight is, higher the $T_{L\text{-}D}$ will be.

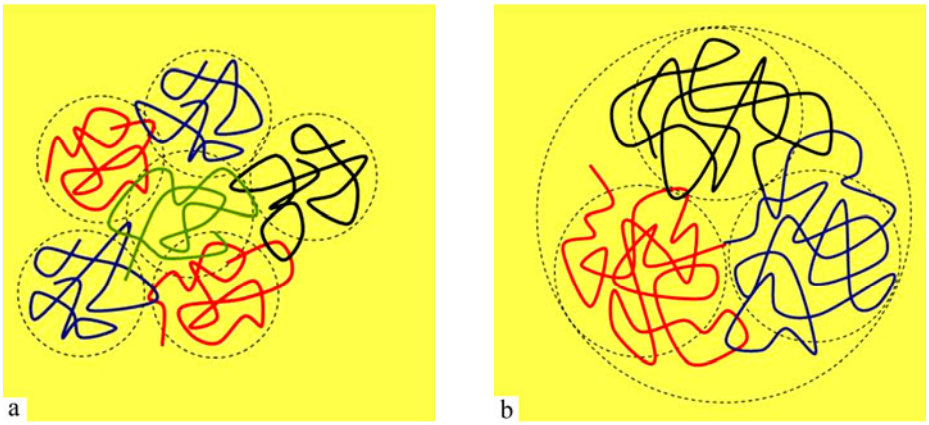

Fig. 9 Proposed 2D blob model of polymer chain(s) with a pancake conformation in the ultrathin film The blob size is molecular-weight-dependent and there is a critical molecular weight. (a) Below the critical molecular weight a polymer chain is within a 2D blob and the blob size increases with molecular weight; (b) Above the critical molecular weight a polymer chain contains several 2D blobs.

In this study we proposed a 2D blob model of polymer chain(s) with a "pancake" conformation in the ultrathin film to explain the molecular weight dependence of $T_{L\text{-}D}$ transition as shown in Fig. 9[14]. The key factor is that the polymer chains within the blob "passively" diffuse jointly cross the depletion zone in-between a growing crystal and an amorphous layer. It is significant to note that the blob size is molecular-weight-dependent and there is a critical molecular weight. Below the critical molecular weight a polymer chain is within a 2D blob, thus the blob size increases with molecular weight, as schematically shown in Fig. 9(a). Above the critical molecular weight a polymer chain may contain several 2D blobs, thus the blob size no longer increases with molecular weight, as schematically shown in Fig. 9(b). In this case b the diffusion of a polymer chain within a blob is relatively independent. In the PEO system studied the critical molecular weight is about 253000 g/mol. When M_w < 253000 g/mol, $T_{L\text{-}D}$ rapidly increases with increasing M_w and when M_w > 253000 g/mol, $T_{L\text{-}D}$ asymptotically approaches to $T_{L\text{-}D}(\infty)$.

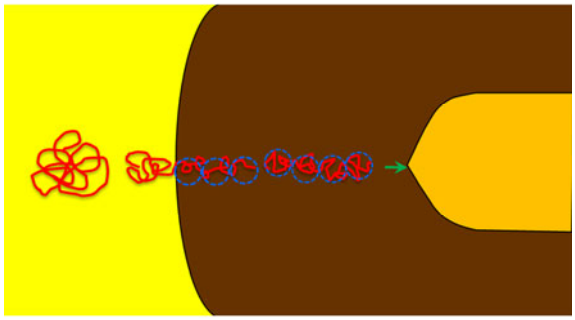

Fig. 10 Partially un-entangled polymer chain crawling across the depletion zone towards the crystal

For the molecular weight dependence of $T_{D\text{-}F}$, the critical molecular weight is $M_w \approx 27000$ g/mol. The most important feature in $T_{D\text{-}F}$ transition is that polymer chains must diffuse across a wide depletion zone to join crystals. Considering sliding motion feature of polymer chains, we proposed another blob model to explain how a partially un-entangled polymer chain crawls across the depletion zone towards the crystal (Fig. 10). The circles in the figure highlight individual blobs. When $M_w < 27000$ g/mol a polymer chain within a blob diffuses across the depletion zone independently, thus $T_{D\text{-}F}$ increase with increasing M_w. When $M_w > 27000$ g/mol, a polymer chain contains a few blobs. They form a blob string to diffuse across the depletion zone cooperatively, thus $T_{D\text{-}F}$ asymptotically approaches to $T_{D\text{-}F}(\infty)$.

CONCLUSIONS

In summary, we conducted experimental observations on labyrinthine, dendritic and faceted crystal patterns formed in ultrathin films of six poly(ethylene oxide) fractions with molecular weights from 25000 g/mol to 932000 g/mol within a crystallization temperature range from 20 °C to 60 °C. We found the labyrinthine-to-dendritic transition attributed to a change from a local-diffusion to diffusion-limited-aggregation (DLA) and the dendritic-to-faceted transition attributed to a turnover of the pattern formation mechanism from DLA to crystallization control. Then we quantitatively distinguished the labyrinthine-to-dendritic and dendritic-to-faceted transition temperatures $T_{L\text{-}D}$ and $T_{D\text{-}F}$ through systematical studies on changes in periodicity and in fractal dimension. Finally we obtained the molecular weight dependences of $T_{L\text{-}D}$ and $T_{D\text{-}F}$ as: $T_{L\text{-}D}(M_w) = T_{L\text{-}D}(\infty) - K_{L\text{-}D} / M_w$, where $T_{L\text{-}D}(\infty)$ = 38.2 °C and $K_{L\text{-}D}$ = 253000 °C·g/mol and $T_{D\text{-}F}(M_w) = T_{D\text{-}F}(\infty) - K_{D\text{-}F} / M_w$, where $T_{D\text{-}F}(\infty)$ = 54.7 °C and $K_{D\text{-}F}$ = 27000 °C·g/mol. In this study we proposed quasi two-dimensional blob models to provide empirical explanations of the molecular weight dependences. The key factor is that the polymer chains within a blob diffuse jointly cross the depletion zone in-between a growing crystal and an amorphous layer. Another key factor is that the blob size is molecular-weight-dependent and there is a critical molecular weight. Below the critical molecular weight a polymer chain is within the 2D blob, thus the blob size increases with molecular weight, the transition temperature rapidly increases with the molecular weight. Above the critical molecular weight a polymer chain may contain several 2D blobs, the blob size no longer increases with molecular weight, thus the transition temperature asymptotically approaches to the maximum transition temperature. These molecular weight dependences reveal the macromolecular effect on the pattern formation and selection of crystalline polymers.

REFERENCES

1 Rubinstein, M. and Colby, R., "Polymer physics", Oxford University Press, Oxford, 2003
2 Fox, T.G. and Flory, P.J., J. Appl. Phys., 1950, 21: 581
3 Wunderlich, B., "Macromolecular physics, Vol. 1, 2 and 3", Academic, New York, 1973, 1976, 1980
4 Armistead, K. and Goldbeck-Wood, G., Adv. Polym. Sci., 1992, 100: 219
5 Cheng, S.Z.D., "Phase transitions in polymers: the role of metastable states", Elsevier Science, Amsterdan, 2008
6 Wunderlich, B., J. Chem. Phys., 1958, 29: 1395
7 Keith, H.D. and Padden, F.J., J Appl. Phys., 1963, 34: 2409
8 Keith, H.D. and Padden, F.J., J. Appl. Phys., 1964, 35: 1270
9 Keith, H.D. and Padden, F.J., J. Appl. Phys., 1964, 35: 1286
10 Stamm, M., Fischer, E.W., Deftenmaier, M. and Convert, P., Faraday Disscuss. Chem. Soc., 1979, 68: 376
11 Cheng, S.Z.D. and Wunderlich, B., J. Polym. Sci., Part B: Polym. Phys., 1986, 24:577
12 Cheng, S.Z.D., Barley, J.S. and Meerwall, E.D.V., J. Polym. Sci., Part B: Polym. Phys., 1991, 29: 515
13 Sakai, Y., Imai, M., Kaji, K. and Tsuji, M., Macromolecules, 1996, 29: 8830
14 Zhang, G., Jin, L., Zheng, P., Shi, A.C. and Wang, W., Polymer, 2010, 51: 554

15 Brener, E.A. and Temkin, D.E., Europhys. Lett., 1989, 10: 171
16 Galenko, P.K. and Krivilyov, M.D., Modelling Simul. Mater. Sci. Eng., 2000, 8: 81
17 Shibkov, A.A., Zheltov, M.A., Korolev, A.A., Kazakov, A.A. and Leonov, A.A., J. Crystal Growth, 2005, 285: 215
18 Frank, C.W., Rao, V., Despotopoulou, M.M., Pease, R.F.W., Hinsberg, W.D., Miller, R.D. and Rabolt, J.F., Science, 1996, 273: 912
19 Reiter, G. and Sommer, J.U., Phys. Rev. Lett., 1998, 80: 3771, J. Chem. Phys., 2000, 112: 4376
20 Taguchi, K., Miyaji, H., Izumi, K., Hoshino, A., Miyamoto, Y. and Kokawa, R., Polymer, 2001, 42: 7443
21 Li, L., Chan, C.M., Yeung, K.L., J.H.L., Ng, K.M. and Lei, Y., Macromolecules, 2001, 34: 316
22 Zhang, F., Liu, J., Huang, H., Du, B. and He, T., Eur. Phys. J. E., 2002, 8: 289
23 Jiang, Y., Yan, D.D., Gao, X., Han, C.C., Jin, X.G. and Li, L., Macromolecules, 2003, 36: 3652
24 Kikkawa, Y., Abe, H., Fujita, M., Iwata, T., Inoue, Y. and Doi, Y., Macromol. Chem. Phys., 2003, 204: 1822
25 Mareau, V.H. and Prud'homme, R.E., Macromolecules, 2005, 38: 398
26 Zhai, X.M., Wang, W., Ma, Z.P., Wen, X.J., Yuan, F., Tang, X. F. and He, B.L., Macromolecules, 2005, 38: 1717
27 Zhai, X., Wang, W., Zhang, G. and He, B., Macromolecules, 2006, 39: 324
28 Zhu, D.S., Liu, Y.X., Chen, E.Q., Li, M., Chen, C., Sun, Y.H., Shi, A.C., Van Horn, R.M. and Chen, S.Z.D., Macromolecules, 2007, 40: 1570
29 Ma, Z.P., Zhang, G.L., Zhai, X.M., Jin, L.X., Tang, X.F., Zheng, P. and Wang, W., Polymer, 2008, 49: 1629
30 Zhang, G.L., Jin, L.X., Ma, Z.P., Zhai, X.M., Yang, M., Zheng, P., Wang, W. and Wegner, G., J. Chem. Phys., 2008, 129: 224708
31 Zhang, G.L., Cao, Y., Jin, L.X., Zheng, P. Van Horn, R.M., Lotz, B., Cheng, S.Z.D. and Wang, W., Polymer, 2011, 52: 1133
32 Zhang, G., Zhai, X., Ma, Z., Jin, L., Zheng, P., Wang, W., Cheng, S.Z.D. and Lotz, B., ACS Macro Lett., 2012, 1: 217
33 Zhang, G.L., Wen, X.J., Zhai, X.M. and Wang, W., Acta Polymerica Sinica (in Chinese), 2013, (3): 398
34 Jeon, K. and Krishnamoorti, R., Macromolecules, 2008, 41: 7131
35 Liang, Y., Zheng, M., Park, K.H. and Lee, H.S., Polymer, 2008, 49: 1961
36 Wang, Y., Chan, C.M., Ng, K.M. and Li, L., Macromolecules, 2008, 41: 2548
37 Jin, L., Zhang, G., Zhai, X., Ma, Z., Zheng, P. and Wang, W., Polymer, 2009, 50: 6157
38 Liu, Y.X., Li, J.F., Zhu, D.S., Chen, E.Q. and Zhang, H.D., Macromolecules, 2009, 42: 2886
39 Liu, Y.X. and Chen, E.Q., Coord. Chem. Rev., 2010, 254: 1011
40 Lovinger, A.J. and Cais, R.E., Macromolecules, 1984, 17: 1939
41 Witten, T.A. and Sander, L.M., Phys. Rev. Lett., 1981, 47: 1400
42 Brener, E., Müller-Krumbhaar, H. and Temkin, D., Phys. Rev. E, 1996, 54: 2714
43 Faucher, J.A., Koleske, J.V., Santee, E.R., Stratta, J.J. and Wilson, C.W., J. Appl. Phys., 1966, 37: 3962
44 Sukhishvili, S.A., Chen, Y., Müller, J.D., Gratton, E., Schweizer, K.S. and Granick, S., Nature (London), 2000, 406: 146
45 Mullins, W.W. and Sekerka, R.F., J. Appl. Phys., 1964, 35: 444
46 Langer, J.S., Rev. Mod. Phys., 1980, 52: 1
47 Goldenfeld, N.J., Cryst. Growth, 1987, 84: 601
48 Schönherr, H. and Frank C.W., Macromolecules, 2003, 36: 1199